

Probabilistic Hysteresis in Integrable and Chaotic Isolated Hamiltonian Systems

Ralf Bürkle¹,[✉] Amichay Vardi,² Doron Cohen,³ and James R. Anglin¹

¹State Research Center OPTIMAS and Fachbereich Physik, Technische Universität Kaiserslautern, D-67663 Kaiserslautern, Germany

²Department of Chemistry, Ben-Gurion University of the Negev, Beer-Sheva 84105, Israel

³Department of Physics, Ben-Gurion University of the Negev, Beer-Sheva 84105, Israel

 (Received 31 March 2019; revised manuscript received 3 July 2019; published 13 September 2019)

We propose currently feasible experiments using small, isolated systems of ultracold atoms to investigate the effects of dynamical chaos in the microscopic onset of irreversibility. A control parameter is tuned past a critical value, then back to its initial value; hysteresis appears as a finite probability that the atoms fail to return to their initial state even when the parameter sweep is arbitrarily slow. We show that an episode of chaotic dynamics during part of the sweep time produces distinctive features in the distribution of final states that will be clearly observable in experiments.

DOI: [10.1103/PhysRevLett.123.114101](https://doi.org/10.1103/PhysRevLett.123.114101)

In macroscopic systems, irreversible evolution involves an increase of entropy. As, for example, in the rapid expansion of a gas behind a moving piston, the system's phase-space ensemble spreads among instantaneous energy surfaces, thereby spreading *into* a larger region of phase space. Ergodization due to dynamical chaos is then invoked to say that the ensemble effectively *fills* this larger region at a reduced coarse-grained density, so that entropy increases even though Liouville's theorem forbids phase-space volume change in isolated systems.

A striking form of irreversibility can be observed in hysteresis experiments: A control parameter is slowly changed and then changed back to its initial value, and yet the system does not return to its initial state. Recent experiments have studied hysteresis in dissipative open systems [1,2]. In this Letter, we discover a new mechanism for irreversibility in *isolated* systems, which we call Hamiltonian hysteresis. This mechanism is related to topological structure in phase space.

The standard mechanism for irreversibility, as in the piston paradigm, is based on the linear response (Kubo) theory for dissipation. For an isolated system, this theory requires the assumption of chaos, as outlined by Ott and co-workers [3–5], Wilkinson [6,7], and Cohen [8]. The standard theory forbids quasistatic entropy growth, because linear response, by definition, provides zero energy spreading in the adiabatic limit. In contrast, Hamiltonian hysteresis can provide irreversibility even in the quasistatic limit.

Hamiltonian hysteresis can occur probabilistically even without chaos [9]. Chaos does, however, greatly enhance irreversibility and has observable signatures, as we demonstrate in a small isolated system. We propose to extend recently suggested experiments [9,10] to show these fingerprints of chaos in irreversibility. In particular, we (i) explain how irreversibility can arise even in quasi-integrable dynamics, (ii) identify fingerprints of quasistatic passage

through chaos [10], and (iii) distinguish these from the effects of Kubo-Ott energy spreading for nonzero sweep rates.

Hamiltonian hysteresis.—A simple example of Hamiltonian hysteresis is provided by a classical particle in a double well, where the relative depths of the two wells are slowly tuned over time. If the particle is initially orbiting within the lowest well, it stays within this well adiabatically until the slowly time-dependent well becomes so shallow that the particle escapes over the interwell potential barrier. When there is no dissipation from a macroscopic reservoir to drag the particle down to the bottom of the second well (as, for example, in [2]), the particle continues flying above the barrier, back and forth across both wells. If the relative depths of the two wells are then slowly returned to their initial values, however, there is a subtlety in adiabatic mechanics involving the breakdown of adiabaticity around a separatrix even for an arbitrarily slow change of parameters [11–15]. Whether the particle ends up orbiting within the original well after this, or is instead found in the other well, turns out to depend sensitively on the phase of the particle in its initial orbit, as well as on the timing of the potential change. If these are not both controlled to high precision, it will be probabilistic whether the particle ends up back in its initial state or in a dramatically different one [9,16–20].

A system similar to the double well, but which can include quantum many-body effects and also be realized experimentally, is the two-mode Bose-Hubbard model (“dimer”). In [9] we showed how probabilistic hysteresis in such an integrable Hamiltonian system can be described quantitatively in terms of expanding and filling phase-space volumes, just as in the usual statistical mechanical theory, showing that this simple hysteresis is truly a microscopic limit of macroscopic irreversibility. To investigate the role of dynamical chaos in the microscopic onset of

irreversibility, we now turn to a class of realizable model systems that can be tuned to be either integrable or chaotic: the three-site Bose-Hubbard “trimer”.

Proposed experiments.—Our testing ground system consists of N condensed bosons in an optical lattice with three sites. In the tight-binding Bose-Hubbard limit, its Hamiltonian is

$$\hat{H} = \frac{x(t)}{2}(\hat{n}_1 - \hat{n}_3) + \frac{U}{2} \sum_{j=1}^3 \hat{n}_j^2 - \frac{\Omega}{2} \sum_{j=1}^2 (\hat{a}_{j+1}^\dagger \hat{a}_j + \text{H.c.}). \quad (1)$$

Here $\hat{n}_j = \hat{a}_j^\dagger \hat{a}_j$ are the occupations of the j th site, $U < 0$ is the attractive on site interaction, and Ω is the intersite hopping frequency. The external parameter $x(t)$ controls the potential bias. Our hysteresis scenario is the forward-and-back sweep

$$x(t) = x_0 + (x_I - x_0) \frac{|t|}{T}, \quad -T < t < T. \quad (2)$$

The control parameter $x(t)$ is swept from x_I at the initial time $t = -T$ to x_0 at $t = 0$, and then swept back to x_I at $t = +T$, with a sweep rate $\dot{x} \propto 1/T$.

We assume negative x_I large enough that for early and late times hopping between sites is adiabatically suppressed (they are far detuned). During these initial and final stages, therefore, the three occupation numbers \hat{n}_j are adiabatically invariant and evolution is trivial. With large $-x_I$ we assume that an initial state can be prepared at $t = -T$, which is cold enough that most atoms are in the lowest-energy site $j = 1$. We do *not* require an initial coherent state of definite phase, but a low-temperature thermal mixed state. To simplify our explanation of the subsequent evolution, we idealize this realistic state as a narrow, low-energy microcanonical state. A more realistic canonical distribution will show similar behavior, just with a larger range of energies. The data that will show hysteresis will be the occupation numbers \hat{n}_j , measured at $t = +T$ and recorded for many runs (repeated or parallel) of the experiment. High-precision atom counting is not required because the final states that must be distinguished differ by significant numbers. Both state preparation and final readout are performed at times when the system dynamics is trivial, and so both are cleanly separated as physical processes from the nontrivial dynamics that they allow us to see.

Simulated results.—Throughout this Letter, we describe the quantum many-body evolution of our Bose-Hubbard system in the semiclassical truncated Wigner approximation, evolving an initial ensemble representing the quantum mixed state with the Gross-Pitaevskii equation (discrete nonlinear Schrödinger equation) that is associated with Eq. (1) [21]. This approximation should be accurate for attainably large particle numbers N .

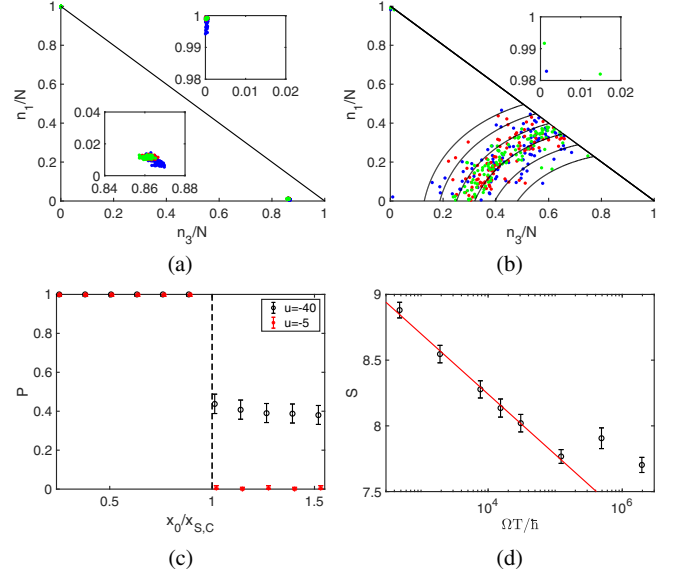


FIG. 1. Simulations of Hamiltonian hysteresis with Eq. (1). The occupations (n_1, n_3) at the end of the sweep protocol Eq. (2). (Upper) Each dot represents a separate run of the experiment. (Insets) Enlargements of the relevant regions (upper-left and lower-right corners) to show the time dependence of the size of the cloud in (a) and the very low return probability in (b). Different colors correspond to different sweep rates: (a) For $u = -40$, with $x_I/\Omega = -100$ and $x_0/\Omega = 60$ (blue: $\Omega T/\hbar = 5333$, red: $\Omega T/\hbar = 53333$, green: $\Omega T/\hbar = 106667$). (b) For $u = -5$, with $x_I/\Omega = -40$ and $x_0/\Omega = 6$ (blue: $\Omega T/\hbar = 7667$, red: $\Omega T/\hbar = 30667$, green: $\Omega T/\hbar = 122667$). The black curves are contours of constant energy just after the exit from chaos (for details, see Supplemental Material [21]). Different contours correspond to different energies. (c) Return probabilities $P(x_0)$ defined as the fraction of 400 runs that comes back to the initial distribution. (d) Dependence of the entropy S (log area of the n distribution) on the sweep time T for simulations in case (b). The red line shows a fit to $-a \log(\Omega T/\hbar) + S_0$ before S levels off to a residual value. For the simulation in (a), the width of the distribution is negligible.

Numerical results simulating Hamiltonian hysteresis for two representative values of the interaction parameter $u = UN/\Omega$ are shown in Fig. 1. Measurements of $n_{1,3}$ in the initial state at $t = -T$ will show a distribution like that shown in Figs. 1(a) and 1(b): Almost all atoms are in site 1. If x_0 is below a critical value x_S when $u = -40$, or below a threshold x_C when $u = -5$, the system returns to its initial state at $t = +T$. However, if the parameter sweep extends beyond these thresholds, some experimental runs end up in significantly different states with different $n_{1,3}$. We define the fraction of runs in which the final $n_{1,3}$ populations are indistinguishable from their initial values to be the measured return probability $P(x_0)$. Dramatic differences are observed between the post-threshold final population distributions of Figs. 1(a) and 1(b). Whereas the final $n_{1,3}$ values for $u = -40$ are nearly binary, i.e., tightly localized around either the original values or around a

single alternative, the $n_{1,3}$ ensemble for $u = -5$ traces a strip whose width becomes smaller as the sweep becomes slower. Rather than vanish in the limit of an infinitely slow sweep, the strip's width saturates to a finite value, implying a significant final-state entropy.

In what follows, we show that these observations provide a clear and experimentally observable hallmark of chaos in Hamiltonian hysteresis. For $u = -40$, the classical dynamics of Eq. (1) remains integrable throughout our hysteresis scenario. Irreversibility is then generated by essentially the same mechanism that produces it in the double-well example above or in the Bose-Hubbard dimer [9]. Here it is the simple merging, at $x = x_S$, of two tori in phase space [21]. By contrast, for $u = -5$, the classical dynamics becomes chaotic at $x > x_C$, with dramatic effects on the final n_j distribution [21].

Phase-space structure.—Discounting the conserved total particle number N , the Bose-Hubbard trimer has 2 degrees of freedom, with two pairs of canonical variables (q_1, q_2, p_1, p_2) spanning its phase space [21]. Energy surfaces are therefore 3D and the dynamics in any given region of phase space can be either quasi-integrable or chaotic, depending on the values of u and x . In the integrable regions of phase space, we can define action angle variables (I_a, φ_a) and (I_b, φ_b) , so that the quasistatic motion at any given value of x takes place on the surface of the 2D tori defined by the actions $I_{a,b}$. Each 3D energy surface consists of multiple tori, all satisfying $H(I_a, I_b; x) = E$.

Different types of adiabaticity.—During periods of integrable motion, adiabaticity is maintained in the Einstein-Landau sense [22], as the conservation of $I_{a,b}$ under sufficiently slow variation of x . In our scenario, this means that $1/T \ll \omega_B$, where ω_B are the perturbative Bogoliubov frequencies around the followed stationary point [21]. The system remains on a single $\mathbf{I} \equiv (I_a, I_b)$ torus whose energy changes as $E(t) = H[\mathbf{I}; x(t)]$. By contrast, when the dynamics becomes chaotic, the I_a and I_b motions become coupled and can exchange energy. Rather than follow a single torus, the system is then free to ergodize over the entire 3D energy surface (or over the chaotic part of a mixed energy surface). As long as chaos prevails, the system's energy will follow the adiabatic energy surface, as discussed by Ott [3]. Unlike in integrable adiabaticity where the two actions are adiabatic invariants, the single adiabatic invariant in the Ott regime is the enclosed phase-space volume.

While the actions $I_{a,b}$ are generally rather complex functions of the canonical variables $q_{1,2}, p_{1,2}$, their form at $t = \pm T$ is quite simple: They correspond closely to the measured populations $n_{1,3}$. Furthermore, since the actions do not change during integrable motion, our final population distribution can be considered a snapshot of the action distribution upon exit from the Ott regime.

Quasi-integrable scenario.—Analyzing the Hamiltonian hysteresis scenario for $u = -40$, we find that the dynamics remains quasi-integrable throughout the process [21]. This is illustrated in the Poincaré sections of Fig. 2(a) at representative x values [21]. All black points within a given section have the same energy E . The magenta points indicate the quasistatic evolution, at each value of x , of those points in our actual ensemble with energy near E . Since energy is not a constant of motion, several E sections are required in order to illustrate the ensemble at a given moment. The time-dependent energy for some of the ensemble trajectories is plotted as well. During the forward sweep, the evolving trajectories remain restricted to the initially occupied torus \mathbf{I}^0 . Beyond $x = x_S$ the occupied torus merges with another (empty) torus \mathbf{I}^1 . When $x = x_S$ is crossed again on the backward sweep, the ensemble splits between the two tori $\mathbf{I}^{0,1}$. Subsequently, the two subensembles evolve to different energies, as implied by Einstein-Landau adiabaticity, namely, $E(t) = H[\mathbf{I}^k; x(t)]$. Those trajectories that come back to the initial torus \mathbf{I}^0 contribute to $P(x_0)$. Their fraction can be determined by the Kruskal-Neishtadt-Henrard theorem [9,16–20].

Passage through chaos scenario.—Analyzing the Hamiltonian hysteresis scenario for $u = -5$, we observe in the Poincaré sections of Fig. 2(b) that for $x > x_C$ the initially regular orbits around an energy minimum merge into a chaotic zone [21]. The ensemble trajectories spread ergodically throughout this chaotic zone, which is a section of a three-dimensional phase-space region within the energy shell. On the backward sweep, the ergodized ensemble emerges from chaos step by step, gradually breaking into a range of many different integrable tori. Each final torus corresponds to a pair of adiabatically conserved action variables, which at late times can be identified as the occupation numbers $n_{1,3}$.

The scatter of points in Fig. 1(b) is thus the direct experimental signal of the spreading of the ensemble into many tori after passage through chaos, while Fig. 1(a) shows the two final tori of the integrable scenario. The larger dispersion in phase space due to chaotic ergodization is responsible for the much lower return probabilities $P(x)$ for $x > x_C$ in Fig. 1(c).

Energy spreading.—Had all tori formed at the same detuning $x = x_C$ in the reverse sweep, one would expect that the final distribution in Fig. 1(b) would trace a single contour in the $n_{1,3}$ plane and the energy would spread according to the formula $E(t) = H[\mathbf{I}; x(t)]$, where the actions belong to the surface $H[\mathbf{I}; x_C] = E_C$, with $E_C = H[\mathbf{I}^0; x_C]$ that corresponds to the initially occupied torus. However, the transition from chaos to integrability is gradual, occurring over an intermediate mixed-phase-space interval during which integrable tori are formed one by one within the chaotic sea. Accordingly, each torus joins a different energy shell as it becomes Einstein-Landau adiabatic. Some of these newly formed tori may later

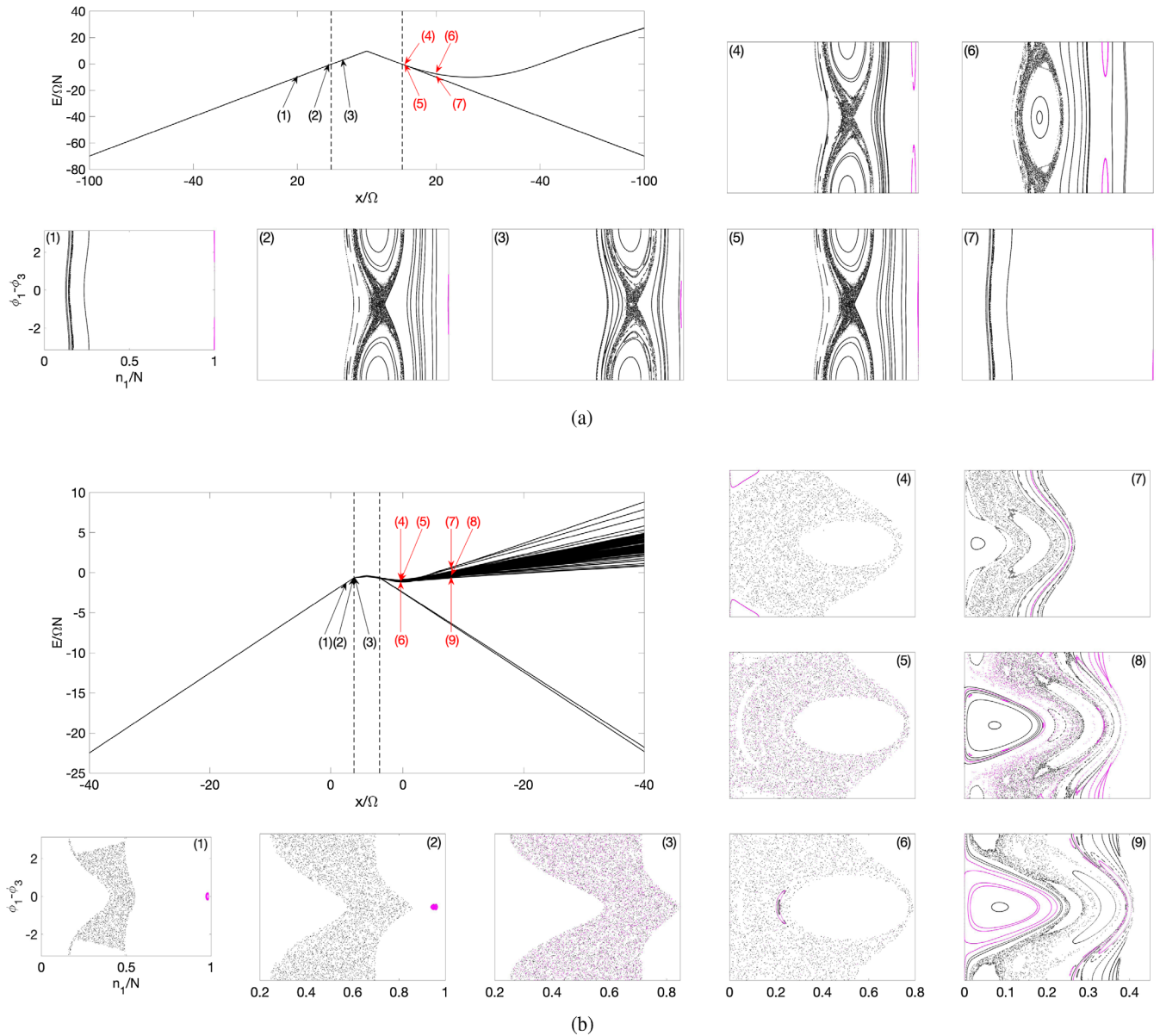


FIG. 2. Evolution of an ensemble of trajectories for (a) $u = -40$ and (b) $u = -5$. The upper-left plot in each set shows the time-dependent energies of the ensemble trajectories vs $x(t)$. The vertical dashed lines indicate the critical values x_S and x_C , respectively. Arrows indicate x values for which Poincaré sections are displayed for the forward (black) and backward sweep (red). In the backward sweep, the ensemble is no longer monoenergetic. In (a) just two E sections are required because only two tori are involved, but in (b) a range of energy surfaces is occupied and three representative sections are shown. Black points in the Poincaré sections are monoenergetic trajectories of the instantaneous Hamiltonian, while the magenta points show actual ensemble points within a narrow range of energies, evolving for several orbits under the instantaneous Hamiltonian.

merge into chaos again, so that a trajectory may undergo several transitions from Ott to Einstein-Landau adiabaticity and back before it finally emerges from chaos. Thus the action distribution on the final exit from chaos is observed to have an *intrinsic* energy width due to the gradual nature of the transition, even if the sweep is infinitely slow.

After the final exit from chaos, energies spread out adiabatically according to the formula $E(t) = H[\mathbf{I}; x(t)]$, where the actions \mathbf{I} are conserved. This Einstein-Landau-

adiabatic spreading of energy is not irreversible. The energy contours shown in Fig. 1(b) are those of the Hamiltonian just after exit from chaos, however (see Supplemental Material [21]). Indeed, the plotted $n_{1,3}$ distribution in Fig. 1(b) corresponds to a broadened energy shell whose width decreases as the sweep becomes more adiabatic, but saturates to a finite value in the limit of an infinitely slow sweep [Fig. 1(d)]. Between this intrinsic energy width and ergodic spreading along energy contours,

the final ensemble after Hamiltonian hysteresis with chaos has the substantial entropy shown in Fig. 1(d) [21].

If the sweep is slow, but not strictly adiabatic, there will be additional energy spreading ΔE . Under Einstein-Landau adiabaticity, the spreading is negligible [$\sim \exp(-1/|\dot{x}|)$], but for fully developed chaos Ott's theory predicts diffusion in energy, namely, $\Delta E^2 \propto \dot{x}^{2a}$ with $a = 1$, as opposed to the transient ballistic value $a = 2$. The duration of our "sweep through chaos" is $t \propto T = (|x_f| + x_0)/|\dot{x}|$; hence, we expect $\Delta E \propto |\dot{x}|^a$ with $a = 1 - \alpha/2$. The numerical data of Fig. 1(d) fit the value of $a \sim 0.2$, which is between the $a = 0$ of ballistic dynamics and the $a = 0.5$ that would be expected in the diffusive case, before it levels off. The plateau that is observed for small \dot{x} (large T) indicates that the quasistatic regime has been reached.

Conclusion and outlook.—Experiments like those we have simulated will be able to show the decisive role of chaos right from the microscopic onset of irreversibility in small isolated systems, by observing the dramatic dependence of final n_j distributions and the associated return probability P on x_0 , on u , and on sweep rate. Quantum corrections to the semiclassical results at smaller particle numbers warrant future investigation.

R. B. and J. R. A. acknowledge support from State Research Center OPTIMAS and the Deutsche Forschungsgemeinschaft (DFG) through SFB/TR185 (OSCAR), Project No. 277625399. A. V. and D. C. acknowledge support by the Israel Science Foundation (Grant No. 283/18).

-
- [1] S. Eckel, J. G. Lee, F. Jendrzejewski, N. Murray, C. W. Clark, C. J. Lobb, W. D. Phillips, M. Edwards, and G. K. Campbell, Hysteresis in a quantized superfluid 'atomtronic' circuit, *Nature (London)* **506**, 200 (2014).
- [2] A. Trenkwalder *et al.*, Quantum phase transitions with parity-symmetry breaking and hysteresis, *Nat. Phys.* **12**, 826 (2016).
- [3] E. Ott, Goodness of Ergodic Adiabatic Invariants, *Phys. Rev. Lett.* **42**, 1628 (1979).
- [4] R. Brown, E. Ott, and C. Grebogi, Ergodic Adiabatic Invariants of Chaotic Systems, *Phys. Rev. Lett.* **59**, 1173 (1987).
- [5] R. Brown, E. Ott, and C. Grebogi, The goodness of ergodic adiabatic invariants, *J. Stat. Phys.* **49**, 511 (1987).
- [6] M. Wilkinson, A semiclassical sum rule for matrix elements of classically chaotic systems, *J. Phys. A* **20**, 2415 (1987).
- [7] M. Wilkinson, Statistical aspects of dissipation by Landau-Zener transitions, *J. Phys. A* **21**, 4021 (1988).
- [8] D. Cohen, Chaos and energy spreading for time-dependent Hamiltonians, and the various regimes in the theory of quantum dissipation, *Ann. Phys. (N.Y.)* **283**, 175 (2000).
- [9] R. Bürkle, A. Vardi, D. Cohen, and J. R. Anglin, How to probe the microscopic onset of irreversibility with ultracold atoms, [arXiv:1903.04834](https://arxiv.org/abs/1903.04834).
- [10] A. Dey, D. Cohen, and A. Vardi, Adiabatic Passage through Chaos, *Phys. Rev. Lett.* **121**, 250405 (2018).
- [11] A. V. Timofeev, On the constancy of an adiabatic invariant when the nature of the motion changes, *JETP* **48**, 656 (1978).
- [12] J. R. Cary, D. F. Escande, and J. L. Tennyson, Adiabatic-invariant change due to separatrix crossing, *Phys. Rev. A* **34**, 4256 (1986).
- [13] J. H. Hannay, Accuracy loss of action invariance in adiabatic change of a one-freedom Hamiltonian, *J. Phys. A* **19**, L1067 (1986).
- [14] J. R. Cary and R. T. Skodje, Reaction Probability for Sequential Separatrix Crossings, *Phys. Rev. Lett.* **61**, 1795 (1988).
- [15] Y. Elskens and D. F. Escande, Slowly pulsating separatrices sweep homoclinic tangles where islands must be small: An extension of classical adiabatic theory, *Nonlinearity* **4**, 615 (1991).
- [16] D. Dobbrott and J. M. Greene, Probability of trapping-state transition in a toroidal device, *Phys. Fluids* **14**, 1525 (1971).
- [17] A. I. Neishtadt, Passage through a separatrix in a resonance problem with a slowly-varying parameter, *J. Appl. Math. Mech.* **39**, 594 (1975).
- [18] J. Henrard, Capture into resonance: An extension of the use of adiabatic invariants, *Celest. Mech.* **27**, 3 (1982).
- [19] A. I. Neishtadt, Probability phenomena due to separatrix crossing, *Chaos* **1**, 42 (1991).
- [20] T. Eichmann, E. P. Thesing, and J. R. Anglin, Engineering separatrix volume as a control technique for dynamical transitions, *Phys. Rev. E* **98**, 052216 (2018).
- [21] See Supplemental Material at <http://link.aps.org/supplemental/10.1103/PhysRevLett.123.114101> for phase-space coordinates, stationary points, ensemble points, Poincaré sections, and energy and entropy.
- [22] L. D. Landau and E. M. Lifshitz, in *Mechanics*, 3rd. ed. (Elsevier, New York, 1982), p. 154ff.